Author Manuscript

Author Manuscript

Author Manuscript

Author Manuscript

HHS Public Access

Author manuscript

Neuroimage. Author manuscript; available in PMC 2023 February 08.

Published in final edited form as:

Neuroimage. 2022 December 01; 264: 119727. doi:10.1016/j.neuroimage.2022.119727.

Diffuse excessive high signal intensity in the preterm brain on advanced MRI represents widespread neuropathology☆

Julia E. Kline[a], **Jon Dudley**[b,c], **Venkata Sita Priyanka Illapani**[a], **Hailong Li**[a,b,d], **Beth Kline-Fath**[a,c,d], **Jean Tkach**[a,b,d], **Lili He**[a,b,d], **Weihong Yuan**[a,b,d], **Nehal A. Parikh**[a,e,*]

[a]Neurodevelopmental Disorders Prevention Center, Perinatal Institute, Cincinnati Children's Hospital Medical Center, Cincinnati, OH, United States

[b]Imaging Research Center, Cincinnati Children's Hospital Medical Center, Cincinnati, OH, United States

[c]Department of Radiology, Cincinnati Children's Hospital Medical Center, Cincinnati, OH, United States.

[d]Department of Radiology, University of Cincinnati College of Medicine, Cincinnati, OH, United States

[e]Department of Pediatrics, University of Cincinnati College of Medicine, Cincinnati, OH, United States

Abstract

Preterm brains commonly exhibit elevated signal intensity in the white matter on T2-weighted MRI at term-equivalent age. This signal, known as diffuse excessive high signal intensity (DEHSI) or diffuse white matter abnormality (DWMA) when quantitatively assessed, is associated with abnormal microstructure on diffusion tensor imaging. However, postmortem data are largely lacking and difficult to obtain, and the pathological significance of DEHSI remains in question. In a cohort of 202 infants born preterm at ≤32 weeks gestational age, we leveraged two newer diffusion MRI models – Constrained Spherical Deconvolution (CSD) and neurite orientation dispersion and density index (NODDI) – to better characterize the macro and microstructural

☆ClinicalTrials.gov Identifier: NCT03345069

This is an open access article under the CC BY-NC-ND license (http://creativecommons.org/licenses/by-nc-nd/4.0/)

*Corresponding author at: Professor of Pediatrics, Cincinnati Children's Hospital, 3333 Burnet Ave, MLC 7009, Cincinnati, OH 45229, Nehal.Parikh@cchmc.org (N.A. Parikh).

Credit authorship contribution statement

Julia E. Kline: Data curation, Formal analysis, Writing – original draft, Writing – review & editing, Investigation, Methodology, Resources, Software, Validation, Visualization. **Jon Dudley:** Data curation, Formal analysis, Writing – review & editing, Investigation, Methodology, Resources, Software, Validation, Visualization. **Venkata Sita Priyanka Illapani:** Data curation, Writing – review & editing, Investigation, Methodology. **Hailong Li:** Methodology, Resources, Validation, Writing – review & editing. **Beth Kline-Fath:** Data curation, Writing – review & editing, Investigation, Methodology. **Jean Tkach:** Writing – review & editing, Investigation, Methodology. **Lili He:** Methodology, Resources, Validation, Writing – review & editing. **Weihong Yuan:** Methodology, Resources, Validation, Formal analysis, Writing – review & editing, Supervision. **Nehal A. Parikh:** Conceptualization, Data curation, Formal analysis, Writing – original draft, Writing – review & editing, Funding acquisition, Investigation, Methodology, Project administration, Resources, Software, Validation, Supervision.

Data and code availability statement

Parameter maps used in this study can be found on GitHub (https://github.com/Jekline2/DWMA.git).
Any additional data not included here are available upon request to the corresponding author.

Author Manuscript Author Manuscript Author Manuscript Author Manuscript

properties of DWMA and inform the ongoing debate around the clinical significance of DWMA. With increasing DWMA volume, fiber density broadly decreased throughout the white matter and fiber cross-section decreased in the major sensorimotor tracts. Neurite orientation dispersion decreased in the centrum semiovale, corona radiata, and temporal lobe. These findings provide insight into DWMA's biological underpinnings and demonstrate that it is a serious pathology.

1. Introduction

When the preterm brain is viewed on T2-weighted MRI at term-equivalent age, a hyperintense signal phenomenon is observed in up to 80% of cases (Dyet et al., 2006; Jeon et al., 2012). This elevated signal, which predominantly occurs in the central white matter surrounding the lateral ventricles, has been escribed as diffuse excessive high signal intensity (DEHSI) when qualitatively diagnosed and diffuse white matter abnormality (DWMA) when quantitatively assessed (Li et al., 2021; Parikh et al., 2021). Debate surrounding its etiology and potential pathology has persisted since it was first described by Maalouf et al., 1999). Several investigators have asserted that DEHSI is not pathologic because it lacked correlation with neurodevelopmental outcomes (Brostrom et al., 2016; Calloni et al., 2015; de Bruine et al., 2011; Hart et al., 2011; Jeon et al., 2012; Kidokoro et al., 2011; Leitner et al., 2014; Morel et al., 2021; Rath et al., 2021; Skiold et al., 2012). However, others have linked DEHSI/DWMA with later deficits in cognitive, language, and/or motor ability (Iwata et al., 2007, 2012; Krishnan et al., 2007), especially when assessed quantitatively around term-equivalent age (Parikh et al., 2020a, 2013, 2020c).

In addition to accumulating evidence that DWMA can prognosticate outcomes, the underlying microstructure of DWMA tissue has begun to be characterized. In small studies of preterm infants with DWMA at term, abnormal diffusion properties of the white matter derived from diffusion tensor modeling (Counsell et al., 2006; Skiold et al., 2010) and altered resting state functional connectivity (He and Parikh, 2015) have been documented. In a postmortem case series, our research group found markedly fewer axons and oligodendrocytes in DWMA regions as compared to preterm brains without DWMA (Parikh et al., 2016). The results overlapped greatly with postmortem histopathology from two infants with cystic periventricular leukomalacia, but with a notable lack of micro or macroscopic cellular necrosis in infants with DWMA. Based on these results, we postulated that DWMA is associated with compromised white matter structure arising from both aberrant myelination and sparse axonal development/injury, akin to postmortem findings of diffuse white matter gliosis (Pierson et al., 2007; Volpe, 2009, 2017). Infants with diffuse gliosis typically exhibit a disturbance of early differentiating preoligodendrocytes (e.g., maturational arrest) accompanied by astrogliosis and microgliosis. Like DWMA on MRI, diffuse white matter gliosis is commonly observed at autopsy in up to 80% of preterm infants (Buser et al., 2012; Pierson et al., 2007). Up to half of such infants with diffuse gliosis exhibit associated necrosis centrally, ranging from macroscopic (commonly referred to as cystic periventricular leukomalacia) to microscopic necrosis. The neuroimaging correlate of diffuse white matter gliosis remains in question but is suspected to be DEHSI/DWMA (Volpe, 2017). We recently applied graph theoretical network analysis to diffusion-weighted connectomes and demonstrated that DWMA extent (normalized volume) at term

Author Manuscript Author Manuscript Author Manuscript Author Manuscript

is closely correlated with widespread decreased network efficiency of the preterm brain, independent of known confounders (Kline et al., 2021).

The diffusion tensor (DT) model often used with diffusion MRI (dMRI) assumes a single diffusion process following a Gaussian distribution within each voxel, which it represents as a 3 × 3 symmetrical matrix characterizing water's displacement along the three principal axes. By diagonalizing this matrix, its eigenvectors and eigenvalues are derived (Soares et al., 2013). Mathematically, fractional anisotropy (FA) is the self-normalized variance of the three principal eigenvalues. FA is the most widely used measure of diffusion within biological tissues. Highly-aligned tissues like the brain's white matter have an organized physical barrier, limiting the direction water can diffuse and leading to more anisotropic diffusion profiles and thus higher FA. FA has often been used as a summary measure of white matter integrity (Mukherjee et al., 2001), although more recently this has been viewed as overly reductive. FA changes can be driven by alterations in neurite density, neurite orientation and fanning, myelination, or injury. In regions of DEHSI, FA is reduced and mean diffusivity (MD) and radial diffusivity (RD) are elevated. Axial diffusivity (AD) tends to increase in DEHSI regions, but trends in both directions have been reported in separate regions of the preterm brain (Cheong et al., 2009). In addition to the non-specific nature of FA, the DT model has other known limitations. Its underlying assumption of Gaussian diffusion leads to limited resolution in regions where tissue structures are more complex, such as areas of fanning or crossing fibers or voxels that contain multiple tracts/tissue types.

In recent years, advanced diffusion MRI models have come to fruition that allow more complex and accurate modeling of white matter micro and macrostructure (Dhollander et al., 2021; Jeurissen et al., 2014; Tournier et al., 2004, 2008; Wang et al., 2011; Zhang et al., 2012). These newer models provide additional parameters of tissue complexity, beyond those associated with the DT model. In this study, we leveraged two such well-characterized models, Constrained Spherical Deconvolution (CSD) (Jeurissen et al., 2014; Tournier et al., 2007, 2008) and Neurite Orientation and Dispersion Density Imaging (NODDI) (Zhang et al., 2012), to derive metrics of neurite density, axonal fanning, and white matter tract cross-section, to serve as *in vivo* surrogates of the histopathological features (Jespersen et al., 2012; Jeurissen et al., 2014; Reijmer et al., 2012) accompanying DWMA.

CSD and its associated tractography is seen as an improvement over the DT model, because it is able to delineate regions of crossing fibers with enhanced fidelity. It does so by computing a full fiber orientation distribution (fOD) for each voxel, by modeling the diffusion-weighted signal as the convolution over spherical coordinates of a single fiber response function (the expected signal from a population of fibers with a single orientation) and the fOD. The metrics derived from the CSD model are fiber density (FD), fiber cross-section (FC), and their product, fiber density and cross-section (FDC). Kelly and colleagues showed that compared to full-term children, preterm children had reductions in all three metrics throughout the brain's white matter (Kelly et al., 2020).

The NODDI model differentiates three types of microstructural environments: intra-cellular, extra-cellular, and cerebrospinal fluid (CSF) compartments, in order to better depict the complexity of axons and dendrites *in vivo* (Zhang et al., 2012). In the CSF compartment,

Author Manuscript Author Manuscript Author Manuscript Author Manuscript

diffusion is isotropic and Gaussian. In the extracellular compartment, which is bounded by glia and neurite cell bodies, diffusion is hindered by these structures and is modelled as anisotropic and Gaussian. Finally, the intracellular compartment is modelled as a set of cylinders with radius zero. Diffusion in this compartment is non-Gaussian and is referred to as restricted, as water can diffuse freely only along the axon, while perpendicular diffusion is minimal. The cylinders themselves can be parallel or dispersed, which gives NODDI enhanced flexibility for modelling neurite orientation patterns in areas with large amounts of axonal fanning, such as the centrum semiovale (i.e., the central white matter). The main metrics of the NODDI model are orientation dispersion index (ODI) and neurite density index (NDI). Jespersen et al. (2012) demonstrated that ODI distributions from the NODDI model show excellent agreement with a quantitative Golgi analysis. In a prior study (Batalle et al., 2017) of NODDI parameters in the preterm brain at term, ODI showed a direct positive relationship with gestational age and postmenstrual age at MRI scan. This data is consistent with histopathological evidence of increased axonal fanning and bending with white matter maturation, especially in regions such as the centrum semiovale. As demonstrated in a cohort of preterm children, ODI decreased in the corona radiata with perinatal history of white matter injury (Young et al., 2019). No prior studies have applied CSD or NODDI models to elucidate the neuropathology associated with DWMA.

In a regional cohort of infants born preterm at ≤32 weeks gestational age with high angular resolution diffusion imaging (HARDI) at term, we employed multi-modal modelling of the white matter, automatically derived measures of cortical maturation, and correlated these advanced neuroimaging metrics with objectively-quantified DWMA volume on term T2-weighted MRI. Based on limited past literature (Batalle et al., 2017; Young et al., 2019), we hypothesized that neurite orientation dispersion, neurite/fiber density, fiber cross-section, and fractional anisotropy would all decrease with DWMA extent and that mean, axial, and radial diffusivity would all increase. Last, we hypothesized that DWMA extent would be associated with cortical dysmaturity on term morphometric MRI. Examining all these metrics together should allow us to disentangle the complex nature of DWMA and gain a wholistic understanding of a preterm pathology that has so far eluded researchers.

2. Materials and methods

2.1. Subjects

Between June 2017 and November 2019, we enrolled a regional, prospective cohort of 202 infants born preterm at 32 weeks gestational age (GA) or less from five Greater Cincinnati area level-III NICUs: 1) Cincinnati Children’s Hospital Medical Center, 2) University of Cincinnati Medical Center, 3) Good Samaritan Hospital, 4) Kettering Medical Center, and 5) St. Elizabeth’s Healthcare. Exclusion criteria included congenital brain abnormalities, cyanotic heart disease, chromosomal abnormalities, or moderate to severe brain abnormality (Kidokoro score Kidokoro et al. 2013 8 and above; see below). Infants requiring mechanical ventilation on greater than 50% oxygen beyond 45 weeks post-menstrual age (PMA) were also excluded, as being transported to MRI posed a higher risk. The Cincinnati Children’s Hospital Institutional Review Board approved this study, and reciprocity agreements resulted

Author Manuscript Author Manuscript Author Manuscript Author Manuscript

in approval at the other four sites. A parent or guardian gave written informed consent before each infant was enrolled.

2.2. MRI data acquisition

All participants were imaged between 40- and 44-weeks PMA at Cincinnati Children's Hospital using the same 3T Philips Ingenia scanner (Philips Medical Systems, Best, the Netherlands) with a 32 channel phase array head coil and identical imaging parameters. Infants were fed 30 min prior to MRI and swaddled in a blanket and a vacuum immobilization device (MedVac, CFI Medical Solutions, Fenton, MI) to promote natural sleep without the use of any sedation. Silicone earplugs were applied to protect the infants' ears from scanner noise (Instaputty, E.A.R. Inc, Boulder, CO). Both an experienced neonatal nurse and neonatologist were present in cases requiring positive pressure airway support. The following parameters were used for all scans: b800 diffusion MRI: echo time (TE) 88 ms, repetition time (TR) 6972 ms, flip angle 90°, field of view 160 × 160 mm^2 , matrix 80 × 79, 2 mm contiguous slices, and scan time 5:58 min. 36 directions of diffusion gradients were applied with 4 interspersed b0 images, all acquired with posterior to anterior phase encoding. In a separate acquisition, 4 b0 images were acquired with anterior to posterior phase encoding; b2000 diffusion MRI: TE 88 ms, TR 5073 ms, flip angle 90°, field of view 160 × 160 mm^2 , matrix 80 × 78, slice thickness 2 mm, scan time 6:27 min, multiband factor 2, and SENSE factor 2. 68 directions of diffusion gradients were applied with 7 interspersed b0 images, all acquired with posterior to anterior phase encoding. In a separate acquisition, 6 b0 images were acquired with anterior to posterior phase encoding; axial T2-weighted image: TE 166 ms, TR 18567 ms, flip angle 90°, voxel dimensions 1.0 × 1.0 × 1.0 mm^3 , and scan time 3:43 min; Sagittal 3D T1-weighted scan with magnetization-prepared rapid gradient echo sequence: TE 3.4 ms, TR 7.3 ms, flip angle 11°, voxel dimensions 1.0 × 1.0 × 1.0 mm^3 , and scan time 2:47 min; axial susceptibility weighted image: TE 7.2 ms, TR 29 ms, flip angle 17°, voxel dimensions 0.57 × 0.57 × 1.00 mm^3 , and scan time 3:27 min.

2.3. DWMA quantification

Our recently developed deep learning algorithm (Li et al., 2021) was used to quantify DWMA extent on T2-weighted MRI. Briefly, the algorithm, which utilizes ResU-Net architecture, was trained on ground truth DWMA data generated by our prior semiautomated algorithm (Li et al., 2019) and manually optimized by two human experts. Using an internal cohort of 98 very preterm infants and a two-fold cross-validation scheme, the algorithm achieved a Dice similarity coefficient of 0.91 and a balanced accuracy of 96%, with only marginally lower performance metrics (0.88 and 92%, respectively) when tested on an external cohort (n = 28). DWMA extent was quantified as the number of voxels our algorithm labeled as DWMA multiplied by the voxel size (in mm^3) and normalized (divided) by each infant's total white matter volume (in mm^3), to correct for the effect of differing brain sizes. The mean (SD) normalized DWMA volume for our final cohort was 0.0293 (0.0171), which represents 2.93% of the total white matter. We defined normal DWMA as a volume <1 SD below the mean (0.0122; n = 37) and severe DWMA as normalized DWMA volume >1.28 SD above the mean (i.e., >90th percentile) (0.0683; n = 18), a threshold that has been demonstrated to be independently predictive of motor, cognitive, and language deficits (Parikh et al., 2020a, 2020c).

Author Manuscript Author Manuscript Author Manuscript Author Manuscript

2.4. Brain abnormality scoring

We scored brain abnormality using the system developed by Kidokoro et al. (2013), which sums abnormalities in the cortical grey matter, cerebral white matter, deep grey matter, and cerebellum to generate a single composite score. Of note, this scoring system does not include subjective or objective assessments of DEHSI/DWMA. One pediatric neuroradiologist performed all qualitative and quantitative structural MRI assessments required to generate the Kidokoro score.

2.5. Preprocessing and DT model

We preprocessed the b800 data in FSL (http://fsl.fmrib.ox.ac.uk/fsl/fslwiki/, version 5.0.11). Susceptibility-induced distortions were corrected via FSL's *topup* procedure (Andersson et al., 2003). Eddy current-induced distortions and slice-to-volume movement artifacts were corrected via FSL's *eddy_cuda* (version 9.1) and an Nvidia GPU (Andersson et al., 2017), by estimating changes in the susceptibility-weighted field with subject movement. Slices with average signal intensity more than four standard deviations below the mean were detected and replaced by a non-parametric Gaussian Process prediction (Andersson et al., 2016). From this artifact-corrected data, FSL's *dtifit* function was used to generate maps of FA, MD, RD, and AD.

2.6. CSD model

We processed all b2000 diffusion-weighted data in MRtrix3 (www.mrtrix3.org), a CSD-enabled software (Tournier et al., 2019), using our published methods for preprocessing (PCA denoising, correction for Gibbs ringing; motion artifacts; eddy currents; and the susceptibility-induced off-resonance field, global intensity normalization, and upsampling to 1.3 mm isotropic resolution) (Chandwani et al., 2022). As previously described, we then performed fOD generation via the Tournier algorithm, template construction (using a representative subsample of 40 preterm infants), segmentation of template and subject fODs to produce fixels (a fiber bundle element), warping and registration of individual subject fixels to the template, probabilistic whole-brain tractography, and finally computation of FD, FC, and FDC maps for each subject in template space. As recommended by the creators of CSD, we used the log of FC for all FC analyses, to ensure that the data were centered around zero.

2.7. NODDI model

The b2000 shell was processed identically to the b800 shell, described in the DT processing section. Each shell was then registered to a mid-space using FSL's *midtrans* function, to ensure that both datasets were interpolated the same number of times. The corresponding eddy-rotated b-vector files were adjusted accordingly. To account for the different TRs between the two shells, each preprocessed shell was normalized by dividing by the mean of its corresponding b0 image prior to the concatenation of the two data sets. These combined multi-shell data were processed using the NODDI toolbox (https://www.nitrc.org/projects/noddi_toolbox/), version 1.04. We used the pre-packaged WatsonSHStickTortIsoV_B0 model with default '*invivo*' tissue type settings. Notably, NODDI modelling was first attempted with grid search starting points derived from neonatal data (provided in the

Author Manuscript Author Manuscript Author Manuscript Author Manuscript

toolbox as invivopreterm in the tissue type settings) (Kunz et al., 2014); however, this resulted in failures to converge on a solution.

2.8. dHCP metrics

To examine how DWMA, a white matter signal abnormality, may nonetheless impact early development of the grey matter, we correlated DWMA extent with several global measures of cortical/grey matter maturation automatically derived using the developing human connectome project pipeline (dHCP) (Makropoulos et al., 2018). The dHCP pipeline uses FreeSurfer software to perform template alignment, tissue segmentation, and volume estimation for the neonatal brain. It also calculates regional and global/whole brain values for cortical metrics, including surface area, gyrification index, sulcal depth, and inner cortical curvature (Jeurissen et al., 2014). All T2-weighted MRI images were segmented by the pipeline, and cortical metrics were generated as previously described (Kline et al., 2020a, 2020b; Makropoulos et al., 2018). We analyzed the relationship between DWMA extent and whole-brain sulcal depth, gyrification index, cortical surface area, curvature of the inner cortical surface, and relative volume of the deep nuclear grey matter (raw volume divided by total tissue volume) by fitting a general linear model in Stata (Stata version 16.0, College Station, TX) corrected for (1) PMA at MRI and (2) all covariates of interest. We selected the following covariates for use in all multivariable models: PMA at MRI, gestational age, sex, pneumothorax, bronchopulmonary dysplasia (BPD), retinopathy of prematurity (ROP), maternal milk diet at discharge, caffeine, postnatal steroids, and Kidokoro score, based on our prior research (Parikh et al., 2020b, 2021).

2.9. Statistical analysis

After fitting the three diffusion models and visually inspecting all outputs from the CSD, NODDI, and DTI models, we performed similar analyses for all outcomes of interest. For each outcome metric (FD, FC, FDC, ODI, NDI, FA, MD, RD, AD), our primary statistical analysis involved fitting a general linear model to test the hypothesis (two-tailed) that a significant relationship exists between total DWMA extent and the dMRI metric, after correction for all covariates of interest. Outcomes from the NODDI and DTI models were analyzed using Tract-Based Spatial Statistics (TBSS) (Smith et al., 2006). TBSS can perform voxel-wise statistical analysis in template space of white matter tracts derived from fractional anisotropy maps. Other measures aligned in the same space can also be correlated with an exposure of interest (here DWMA extent). Family-wise error rate correction to control for type I errors was achieved by performing 5,000 permutations of the design matrix to estimate the null distribution. Outcomes from the CSD model were analyzed using connectivity-based fixel enhancement according to the methods of Raffelt (Raffelt et al., 2015), which uses a similar framework to TBSS but is performed on the fixel-level after statistical smoothing. The smoothing process utilizes the probabilistic whole-brain tractograph from CSD to identify fixels that are likely anatomically related, and this information is then used for tract-specific smoothing and statistical enhancement.

We performed an additional analysis statistically comparing average values for each metric of interest in regions marked as DWMA by our algorithm vs all non-DWMA white matter

Author Manuscript Author Manuscript Author Manuscript Author Manuscript

regions. 180 subjects were included in this analysis, and dependent Student's t-tests were used to assess significance.

To identify possible exclusion bias, we compared baseline and clinical characteristics of all included vs excluded subjects. For continuous variables, we used either a Student's t-test or a Mann-Whitney U test, after assessing normality via Shapiro Wilks. We assessed differences in binary variables using Fischer's exact test. This bias analysis was conducted in python, and a p-value of <0.05 indicated significance. Severe bronchopulmonary dysplasia (BPD) was defined as Grade 2 level, which includes nasal cannula >2 L/min or noninvasive positive airway pressure or higher. BPD level was as defined by Jensen et al. (2019) at 36 weeks of PMA. Late-onset sepsis was defined as culture positive blood or cerebrospinal fluid infection after the first week of life. Maternal milk at discharge was defined as any infant feeding with mom's own milk (exclusively or combined with formula) at hospital discharge or time of MRI. Necrotizing enterocolitis (NEC) was defined as proven Bell stage II or III NEC. Severe retinopathy of prematurity (ROP) was defined as ROP stage 3 or worse, or plus disease (enlargement of the posterior veins of the retina and tortuous arterioles) noted in either eye, or need for treatment, including laser, surgery, or Avastin injections.

3. Results

Of the initial cohort of 202 subjects, we excluded 22 subjects: one subject due to ventriculomegaly; a deformation that could compromise warp to the template for CSD/NODDI; four due to artifacts on dMRI that interfered with CSD's global intensity normalization, 15 because they were missing voxels at the periphery of their diffusion-weighted scans (To perform fixel-based analysis, all regions of interest must be present for all subjects), and two due to suboptimal alignment with the fOD template, for a final cohort of 180 for all diffusion model analyses.

Compared to the included subjects, the excluded subjects were born at a later gestational age and higher birth weight. Excluded babies were also more likely to be female (Table 1). There were no other statistically significant differences in baseline variables between the included and excluded infants. Fig. 1 displays a heatmap of locations in the preterm brain where DWMA tended to concentrate for the 180 final subjects.

White matter regions marked as DWMA differed significantly from non-DWMA regions for all metrics examined. With high statistical significance and nearly perfect concordance across subjects (Fig. 2), mean AD, RD, and MD was higher in DWMA voxels compared to non-DWMA voxels ($p < 0.0001$). Average FA, ODI, NDI, FD, and FDC were all significantly lower in DWMA voxels ($p < 0.0001$). Average FC was lower in DWMA voxels, and although the trend was less pronounced than the other metrics, it was still significant ($p = 0.001$).

In the connectivity-based fixel enhancement analysis, FD decreased with DWMA extent throughout the majority of the white matter (Fig. 3), although not in the cerebellum. FC decreased with DWMA extent predominantly in the corticospinal tracts traversing the

Author Manuscript Author Manuscript Author Manuscript Author Manuscript

corona radiata, centrum semiovale, and brainstem and also in the corpus callosum and cerebellum. DWMA extent was associated with a widespread decrease in FDC in nearly all white matter regions, which is to be expected, as FDC generalizes FD and FC. We did not identify any negative associations.

In TBSS analyses of metrics from the NODDI model, NDI decreased with DWMA volume throughout portions of all major white matter regions with the exception of the cerebellum (Fig. 4), in concordance with the FD metric, both of which should approximate the same underlying truth. ODI, on the other hand, decreased in a more localized manner. We detected a large regional ODI decrease with DWMA extent above the lateral ventricles (i.e., centrum semiovale) and in the portion of the corona radiata directly superior. We also identified a small region of ODI decrease in the right temporal lobe.

TBSS analyses of metrics from the DT model detected widespread significant associations between DWMA extent and all four DT metrics. FA decreased while MD, RD, and AD increased with DWMA extent throughout portions of every major white matter tract (Fig. 5).

Of the 180 infants with high-quality dMRI data, 157 had T2 images that were successfully processed using the dHCP pipeline. The pipeline failures were often due to a tiny missing region on the periphery of the structural scan or the reason was indeterminate (‘white-pial error’ reported by the dHCP). Normalized DWMA volume exhibited a positive correlation with curvature of the inner cortex, whether correcting for just PMA (β [95% CI]: 4.34 [2.51, 6.16], p = 2.78e-6) or all covariates of interest (4.52, [2.62, 6.42], p = 2.55e-6). DWMA was also inversely correlated with gyrification index (−1.85 [−3.47, −0.23], p = 0.026) when correcting for PMA, and remained close to significant when correcting for all confounders (−1.68 [−3.38, 0.03], p = 0.054). There were no significant correlations with sulcal depth (9.53 [−19.32, 38.38], p = 0.515) or surface area (−39956.21 [−126910.90, 46998.48], p = 0.365), when correcting for PMA only. The results remained insignificant in multivariable models. Normalized volume of DWMA was also inversely correlated with relative deep nuclear grey matter volume (−0.046 [−0.076, −0.012], p = 0.008) when correcting for PMA, and remained significant when correcting for all confounders (−0.056 [−0.091, −0.021], p = 0.002).

Normalized volume of DWMA did not correlate with white matter abnormality score (r = −0.054; p = 0.477), deep nuclear GM score (r = − 0.055; p = 0.466), cerebellar score (r = −0.033; p = 0.664) or the global brain abnormality score (r = −0.087; p = 0.246). However, it did correlate with cortical GM score (r = −0.168; p=0.024). Severe DWMA did not correlate with global brain abnormality score or any of the four subcomponent scores, including cortical GM score, suggesting DWMA volume is independent of the regional abnormalities that make up the global brain abnormality score.

4. Discussion

We demonstrate that DWMA extent is associated with diffuse micro and macrostructural brain abnormalities in infants born preterm evaluated at term-equivalent age. By combining three separate diffusion MRI models, we can better distinguish the various alterations

Author Manuscript Author Manuscript Author Manuscript Author Manuscript

underlying DWMA pathology in the preterm brain. Our results suggest that on the microscopic level, DWMA is characterized by reduced axonal orientation dispersion primarily in the centrum semiovale (the most common site of DWMA signal) and also in the corona radiata, reduced cross-section of the motor and sensory tracts traversing this region, and widespread reduced fiber density. Our results comparing DWMA vs non-DWMA regions validate pilot studies showing abnormal diffusion metrics and abnormal network connectivity in infants with DWMA (Cheong et al., 2009; Counsell et al., 2006; Skiold et al., 2010). Based on its association with reduced cortical curvature and reduced gyrification, DWMA extent may also be a driver of greater cortical immaturity.

The multimodal insights gained from this study provide the potential biological underpinnings of a prevalent signal abnormality, whose etiology appears multifactorial (Parikh et al., 2020b, 2021), and suggest that DWMA is a serious neuropathology associated with globally compromised white matter morphology and cortical maturational delays. These results are consistent with our group's prior DWMA studies demonstrating its clinical antecedents, postmortem pathology, and significant associations with cognitive, language, and motor impairments at 2 to 3 years corrected age (Parikh et al., 2020a, 2013, 2020b, 2020c, 2016, 2021). These combined results strongly suggest that DWMA is the neuroimaging correlate of diffuse white matter gliosis, the most common postmortem neurological finding reported in 40–80% of very preterm infant deaths (Parikh et al., 2016; Pierson et al., 2007; Volpe, 2009, 2017). Because such a correlate has been lacking, Volpe stated that the functional significance of diffuse white matter gliosis in preterm infants was unknown (Volpe, 2017). Our findings indicate a strong linear relationship between DWMA signal and microscopic white matter alterations that are consistent with diffuse white matter gliosis (Galinsky et al., 2020; Griffith et al., 2012; Volpe, 2009) and, considering the published evidence presented above, underscore its significance as a biomarker of later neurodevelopmental impairment. Studies in infants born very preterm have reported that several regional microstructural metrics are associated with neurodevelopmental deficits at 2 to 3 years corrected age (Ball et al., 2017; Parikh, 2016; Valavani et al., 2021; Vassar et al., 2020). We recently examined the combination of DWMA with structural and functional connectivity and clinical factors and demonstrated that such a multimodal approach was more accurate than individual modalities at predicting cognitive, language, and motor deficits at age two (He et al., 2021). If these results are validated at age three in our ongoing longitudinal cohort study, moderate-severe DWMA should trigger referral for early intervention therapies or neuroprotection trials soon after birth, when the potential for neuroplasticity is maximal.

Our DT model results bear out that DWMA extent indicates compromised white matter morphology. FA typically decreases, accompanied by an increase in the other three DT indices in association with injury mechanisms, disease chronicity, or developmental delay. In the present study, we indeed show that FA broadly decreases with DWMA extent, while the other metrics broadly increase. The fact that these results are consistent throughout the white matter adds to the accumulating evidence that DWMA represents a global brain pathology and validates prior smaller studies (Cheong et al., 2009; Counsell et al., 2006; Skiold et al., 2010). However, as previously mentioned, the DT model oversimplifies inferences about white matter microstructure, and its reliance on just one principal direction negates it

Author Manuscript Author Manuscript Author Manuscript Author Manuscript

applicability in regions of crossing fibers, two limitations not shared by CSD and NODDI (Jespersen et al., 2012; Reijmer et al., 2012).

Data from the CSD and NODDI models allow us to glimpse additional microstructural changes accompanying DWMA. Thus, we can parse the influence of DWMA on two fundamental contributors to the FA parameter (Irzan et al., 2021), neurite density and neurite coherence (defined as 1-ODI) (Batalle et al., 2017). DWMA extent was associated with reduced neurite density (reduced NDI/FD) throughout most of the WM, with the exception of the cerebellum. This bolsters our earlier histopathological analysis showing fewer axons and oligodendroglia cells in DWMA regions (Parikh et al., 2016). It also aligns with our recently-published graph theory analysis in the same cohort, in which DWMA extent was associated with overall decreased global efficiency and decreased local efficiency in brain regions supporting cognitive, linguistic, and motor functions (Kline et al., 2021), likely driven at least in part by this reduced cellularity.

In our current study, DWMA extent was associated with increased neurite coherence (decreased ODI) in a more limited manner, primarily in the centrum semiovale and corona radiata, suggesting that the identified widespread FA decrease is more attributable to reduced neurite density than localized altered neurite coherence. Similarly, Batalle and colleagues concluded that FA's evolution in the developing preterm brain is driven more by increasing neurite density than increasing tract coherence (Batalle et al., 2017). Fiber cross section also decreased with DWMA in a more limited manner. The majority of the FC decreases we detected occurred in the bilateral corticospinal tracts, with additional decreases in the corpus callosum and cerebellum, two crucial motor areas. Based on these regional relationships, we presume that a reduction in neurites due to aberrant maturation or injury likely explains both microstructural findings and also the tight association between DWMA extent with cerebral palsy and lower motor scores at 3 years of age (Parikh et al., 2020a), which we recently reported in very preterm infants. Additionally, all three CSD metrics in similar portions of the preterm brain (e.g., corticospinal tracts and corpus callosum) at term were recently positively correlated with the motor and cognitive sub-test scores of the Bayley Scales of Infant and Toddler Development III assessment tool at ages 1 and 2 years (Pannek et al., 2020).

Paradoxically, the two concomitant microstructural alterations we identified in the central white matter with DWMA, decreased neurite density and localized increased neurite coherence, may have masked the true extent of DWMA's pathology in past studies, especially when viewed through the lens of FA and quantified within the centrum semiovale, the region in which it is most prevalent. The magnitude of the FA parameter is expected to decrease with decreased neurite density but to *increase* with increased neurite coherence, which could have partially disguised the degree of abnormality in DWMA regions. With DWMA, reduced ODI in regions traversed by the corticospinal tracts is likely pathological, reflecting less complex and mature motor pathways.

Few studies have examined the significance and relationship of ODI with preterm birth or perinatal brain injury. In Batalle's very preterm network study (introduced above) (Batalle et al., 2017), streamlines from the CSD model were weighted by metrics from the

Author Manuscript Author Manuscript Author Manuscript Author Manuscript

NODDI model. 1-ODI network weightings showed a negative correlation with gestational age at birth, implying that ODI increased with advancing gestational age. This likely reflects decreased complexity and crossing fibers in the white matter of younger brains (Batalle et al., 2017). Our results validate their findings and suggest that the decrease in ODI we observed with increasing DWMA extent is a result, at least partially, of white matter maturational delay in key regions of crossing fibers. Reduced number of axons and myelination delay can also result from diffuse white matter injury, such as gliosis (Back, 2017). In a study of 6-year-old very preterm born children with a history of perinatal white matter injury, Young et al. reported decreased ODI in the superior corona radiata, similar to our findings in very preterm infants (Young et al., 2019). Thus, localized reduced ODI with DWMA may additionally reflect acute injury. Conversely, two studies in 6 and 7-year-olds concluded that very preterm children exhibit overall increased orientation dispersion compared to term-born children (Kelly et al., 2016; Young et al., 2019). This comparatively higher ODI in preterm children may result from the brain's adaptive response to injury/immaturity and suggests that ODI could be a biomarker of neuroplasticity. Alternatively, these apparently conflicting findings may reflect differences in cohort characteristics, sample size, imaging parameters, and lack of sequence harmonization in one of the two studies (Kelly et al., 2016).

The periventricular spatial distribution of DWMA at term-equivalent age closely matches the early developmental topography of the periventricular crossroads, which is unlikely to be coincidental. Judas et al.(Judas et al., 2005) performed a histological-neuroimaging correlation study in 15 human fetuses and preterm infants between 15- and 36-weeks post-ovulation age and demonstrated that periventricular WM that appears hyperintense on T2 and hypointense on T1-weighted MRI contains periventricular fiber crossroads that comprise callosal, associative, and thalamocortical/corticofugal fibers intersecting in the transverse, sagittal, and radial directions. Furthermore, these regions are rich in extracellular matrix and axonal guidance molecules that likely represent a vulnerable cellular and topographic target. Thus, insults to this vulnerable region can not only disrupt growing axons and premyelinating oligodendrocytes but can also impact the functioning of signaling cascades involved in the preservation and navigation of developing axons. The diversity of fibers traversing the central white matter suggests that insults can result in a range of cognitive, language, and/or sensorimotor impairments (Judas et al., 2005; Parikh et al., 2020a, 2020c). Not surprisingly, the centrum semiovale and frontal/occipital periventricular regions are the most common sites of DEHSI/DWMA in preterm MRI studies and also diffuse white matter gliosis with or without periventricular leukomalacia in postmortem studies (Buser et al., 2012; Pierson et al., 2007). The persistence of this bright signal abnormality in these regions beyond the mid to late fetal stages suggests ongoing immaturity with or without injury to the periventricular fiber crossroads that manifests as DWMA at term-equivalent age. Thus, the most common MRI finding in preterm infants – DWMA – is likely the neuroimaging correlate of diffuse white matter gliosis, the most common postmortem finding in preterm infants (Maalouf et al., 1999; Pierson et al., 2007; Volpe, 2017).

We urgently need mechanistic studies in preterm infants to determine if DWMA is caused by hypoxia-ischemia, nutritional deficiencies, or more likely excessive inflammation, as

Author Manuscript Author Manuscript Author Manuscript Author Manuscript

suggested by recent epidemiologic data (Parikh et al., 2020b, 2021). Additional risk, protective, and mitigating factors that warrant further investigation include maternal milk (Barnett et al., 2018; Blesa et al., 2019; Krishnan et al., 2017a, 2017b; Stoye et al., 2020; Wheater et al., 2022), DNA methylation (Wheater et al., 2022), genetic variation (Krishnan et al., 2017a, 2017b), stress (Stoye et al., 2020), and models that account for multiple perinatal hits (Barnett et al., 2018).

Our analysis of cortical metrics allows us to glimpse how DWMA might influence the developing grey matter. We identified a strong direct relationship between DWMA and inner cortical curvature and an inverse relationship with gyrification index, suggesting that DWMA is associated with delayed cortical maturation. In an independent prospective cohort, we previously showed that cortical curvature is higher in very preterm infants compared to full-term controls (Kline et al., 2019), a result corroborated by the dHCP's developers (Makropoulos et al., 2014). We also demonstrated that increased cortical curvature prognosticates lower language, cognitive (Kline et al., 2020a), and motor scores (Kline et al., 2020b) at two-years corrected age in very preterm infants. We and others have hypothesized that the increased curvature in very preterm groups is based on overall shallower sulci (Kline et al., 2020b; Shimony et al., 2016). However, we did not detect an association between DWMA and sulcal depth in this cohort, but rather a negative association between DWMA and gyrification index, defined as the amount of cortex within the sulcal folds vs the amount of outer visible cortex. This result may lend credence to the tension-based theory of cortical development (Van Essen, 1997), which posits that axons exert a 'pull' on the developing cortex, causing it to fold. We therefore cautiously speculate that the fewer axons available in the white matter of infants with DWMA exert less of a pull, resulting in less cortical gyrification and more curvature. If this is the case, DWMA's high prevalence in preterm populations may partially explain the increased curvature of the preterm brain as compared to full-term newborns. Finally, the decreased volume of deep grey matter identified with DWMA aligns with prior work by Boardman et al. and Srinivasan et al. showing that reduced thalamic volume in very preterm infants at term is cross-sectionally associated with findings of qualitatively defined DEHSI and diffusion changes in regions of DEHSI from the same MRI scans (Boardman et al., 2006; Srinivasan et al., 2007). Thus, another change concomitant with DWMA may explain its strong association with later outcomes.

The major strength of our study was our large and representative cohort size, sampled from academic and non-academic NICUs, our use of an objective and validated measure of DWMA, and the multiple diffusion models employed. Conversely, our study design was limited by the diffusion models themselves, including the previously mentioned limitations of the DT model with regard to resolution of crossing fibers. Furthermore, the NODDI model assumes fixed and identical axonal and extra-axonal diffusivities for all tissues. Deviations from these assumptions that occur with disease states can bias the remaining parameters, resulting in a loss of specificity (Jelescu et al., 2015). Tissue pathology could therefore impart a false change in orientation dispersion or neurite density. However, these weaknesses are partially overcome by combining the three models and examining the overall emergent picture. By doing so, we have devised a more nuanced picture of DWMA microstructural pathology than previously available, one that is unlikely to emerge from

Author Manuscript Author Manuscript Author Manuscript Author Manuscript

large postmortem studies. All correlations reported here were cross-sectional, and future studies should examine such relationships longitudinally.

Our results, especially when combined with our prior reported findings from postmortem histopathology, graph theoretical analysis, epidemiology, and neurodevelopmental prognostic studies, strongly implicate DWMA on term MRI as a significant pathological entity. Our next step is to assess the independent value of DWMA volume in predicting long-term neurodevelopmental impairments from this cohort to validate our prior findings. If validated, future studies should evaluate novel neuroprotective interventions to enhance the quality of life in preterm infants with DWMA.

Acknowledgments

This research was supported by grants R01-NS094200 and R01-NS096037 from the National Institute of Neurological Disorders and Stroke (NINDS), R01-EB029944 from National Institute of Biomedical Imaging and Bioengineering (NIBIB), and R21-HD094085 from the Eunice Shriver Kennedy National Institute of Child Health and Human Development (NICHD). We sincerely thank the parents of infants that participated in our study and the Cincinnati Infant Neurodevelopment Early Prediction Study (CINEPS) Investigators: Principal Investigator: Nehal A. Parikh, DO, MS. Collaborators (in alphabetical order): Mekibib Altaye, PhD, Anita Arnsperger, RRT, Traci Beiersdorfer, RN BSN, Kaley Bridgewater, RT(MR) CNMT, Tanya Cahill, MD, Kim Cecil, PhD, Kent Dietrich, RT, Christen Distler, BSN RNC-NIC, Juanita Dudley, RN BSN, Brianne Georg, BS, Cathy Grisby, RN BSN CCRC, Lacey Haas, RT(MR) CNMT, Karen Harpster, PhD, OT/RL, Lili He, PhD, Scott K. Holland, PhD, V.S. Priyanka Illapani, MS, Kristin Kirker, CRC, Julia E. Kline, PhD, Beth M. Kline-Fath, MD, Hailong Li, PhD, Matt Lanier, RT(MR) RT(R), Stephanie L. Merhar, MD MS, Greg Muthig, BS, Brenda B. Poindexter, MD MS, David Russell, JD, Kari Tepe, BSN RNC-NIC, Leanne Tamm, PhD, Julia Thompson, RN BSN, Jean A. Tkach, PhD, Hui Wang, PhD, Jinghua Wang, PhD, Brynne Williams, RT(MR) CNMT, Kelsey Wineland, RT(MR) CNMT, Sandra Wuertz, RN BSN CCRP, Donna Wuest, AS, Weihong Yuan, PhD.

References

Andersson JL, Skare S, Ashburner J, 2003. How to correct susceptibility distortions in spin-echo echo-planar images: application to diffusion tensor imaging. Neuroimage 20, 870–888. [PubMed: 14568458]

Andersson JLR, Graham MS, Drobnjak I, Zhang H, Filippini N, Bastiani M, 2017. Towards a comprehensive framework for movement and distortion correction of diffusion MR images: Within volume movement. Neuroimage 152, 450–466. [PubMed: 28284799]

Andersson JLR, Graham MS, Zsoldos E, Sotiropoulos SN, 2016. Incorporating outlier detection and replacement into a non-parametric framework for movement and distortion correction of diffusion MR images. Neuroimage 141, 556–572. [PubMed: 27393418]

Back SA, 2017. White matter injury in the preterm infant: pathology and mechanisms. Acta Neuropathol 134, 331–349. [PubMed: 28534077]

Ball G, Aljabar P, Nongena P, Kennea N, Gonzalez-Cinca N, Falconer S, Chew ATM, Harper N, Wurie J, Rutherford MA, Counsell SJ, Edwards AD, 2017. Multimodal image analysis of clinical influences on preterm brain development. Ann. Neurol 82, 233–246. [PubMed: 28719076]

Barnett ML, Tusor N, Ball G, Chew A, Falconer S, Aljabar P, Kimpton JA, Kennea N, Rutherford M, David Edwards A, Counsell SJ, 2018. Exploring the multiple-hit hypothesis of preterm white matter damage using diffusion MRI. Neuroimage Clin 17, 596–606. [PubMed: 29234596]

Batalle D, Hughes EJ, Zhang H, Tournier JD, Tusor N, Aljabar P, Wali L, Alexander DC, Hajnal JV, Nosarti C, Edwards AD, Counsell SJ, 2017. Early development of structural networks and the impact of prematurity on brain connectivity. Neuroimage 149, 379–392. [PubMed: 28153637]

Blesa M, Sullivan G, Anblagan D, Telford EJ, Quigley AJ, Sparrow SA, Serag A, Semple SI, Bastin ME, Boardman JP, 2019. Early breast milk exposure modifies brain connectivity in preterm infants. Neuroimage 184, 431–439. [PubMed: 30240903]

Author Manuscript Author Manuscript Author Manuscript Author Manuscript

Boardman JP, Counsell SJ, Rueckert D, Kapellou O, Bhatia KK, Aljabar P, Hajnal J, Allsop JM, Rutherford MA, Edwards AD, 2006. Abnormal deep grey matter development following preterm birth detected using deformation-based morphometry. Neuroimage 32, 70–78. [PubMed: 16675269]

Brostrom L, Bolk J, Padilla N, Skiold B, Eklof E, Martensson G, Vollmer B, Aden U, 2016. Clinical implications of diffuse excessive high signal intensity (DEHSI) on neonatal MRI in school age children born extremely preterm. PLoS One 11, e0149578. [PubMed: 26886451]

Buser JR, Maire J, Riddle A, Gong X, Nguyen T, Nelson K, Luo NL, Ren J, Struve J, Sherman LS, Miller SP, Chau V, Hendson G, Ballabh P, Grafe MR, Back SA, 2012. Arrested preoligodendrocyte maturation contributes to myelination failure in premature infants. Ann. Neurol. 71, 93–109. [PubMed: 22275256]

Calloni SF, Cinnante CM, Bassi L, Avignone S, Fumagalli M, Bonello L, Consonni D, Picciolini O, Mosca F, Triulzi F, 2015. Neurodevelopmental outcome at 36 months in very low birth weight premature infants with MR diffuse excessive high signal intensity (DEHSI) of cerebral white matter. Radiol. Med 120, 1056–1063. [PubMed: 25903560]

Chandwani R, Harpster K, Kline JE, Mehta V, Wang H, Merhar SL, Schwartz TL, Parikh NA, 2022. Brain microstructural antecedents of visual difficulties in infants born very preterm. Neuroimage Clin 34, 102987. [PubMed: 35290855]

Cheong JL, Thompson DK, Wang HX, Hunt RW, Anderson PJ, Inder TE, Doyle LW, 2009. Abnormal white matter signal on MR imaging is related to abnormal tissue microstructure. AJNR Am. J. Neuroradiol 30, 623–628. [PubMed: 19131414]

Counsell SJ, Shen Y, Boardman JP, Larkman DJ, Kapellou O, Ward P, All-sop JM, Cowan FM, Hajnal JV, Edwards AD, Rutherford MA, 2006. Axial and radial diffusivity in preterm infants who have diffuse white matter changes on magnetic resonance imaging at term-equivalent age. Pediatrics 117, 376–386. [PubMed: 16452356]

de Bruine FT, van den Berg-Huysmans AA, Leijser LM, Rijken M, Steggerda SJ, van der Grond J, van Wezel-Meijler G, 2011. Clinical implications of MR imaging findings in the white matter in very preterm infants: a 2-year follow-up study. Radiology 261, 899–906. [PubMed: 22031710]

Dhollander T, Clemente A, Singh M, Boonstra F, Civier O, Duque JD, Egorova N, Enticott P, Fuelscher I, Gajamange S, Genc S, Gottlieb E, Hyde C, Imms P, Kelly C, Kirkovski M, Kolbe S, Liang X, Malhotra A, Mito R, Poudel G, Silk TJ, Vaughan DN, Zanin J, Raffelt D, Caeyenberghs K, 2021. Fixel-based analysis of diffusion MRI: methods, applications, challenges and opportunities. Neuroimage 241, 118417. [PubMed: 34298083]

Dyet LE, Kennea N, Counsell SJ, Maalouf EF, Ajayi-Obe M, Duggan PJ, Harrison M, Allsop JM, Hajnal J, Herlihy AH, Edwards B, Laroche S, Cowan FM, Rutherford MA, Edwards AD, 2006. Natural history of brain lesions in extremely preterm infants studied with serial magnetic resonance imaging from birth and neurodevelopmental assessment. Pediatrics 118, 536–548. [PubMed: 16882805]

Galinsky R, van de Looij Y, Mitchell N, Dean JM, Dhillon SK, Yamaguchi K, Lear CA, Wassink G, Davidson JO, Nott F, Zahra VA, Kelly SB, King VJ, Sizonenko SV, Bennet L, Gunn AJ, 2020. Magnetic resonance imaging correlates of white matter gliosis and injury in preterm fetal sheep exposed to progressive systemic inflammation. Int. J. Mol. Sci 21 (23), 8891. [PubMed: 33255257]

Griffith JL, Shimony JS, Cousins SA, Rees SE, McCurnin DC, Inder TE, Neil JJ, 2012. MR imaging correlates of white-matter pathology in a preterm baboon model. Pediatr. Res 71, 185–191. [PubMed: 22258130]

Hart A, Whitby E, Wilkinson S, Alladi S, Paley M, Smith M, 2011. Neuro-developmental outcome at 18 months in premature infants with diffuse excessive high signal intensity on MR imaging of the brain. Pediatr. Radiol 41, 1284–1292. [PubMed: 21681616]

He L, Li H, Chen M, Wang J, Altaye M, Dillman JR, Parikh NA, 2021. Deep multimodal learning from MRI and clinical data for early prediction of neurodevelopmental deficits in very preterm infants. Front. Neurosci 15, 753033. [PubMed: 34675773]

He L, Parikh NA, 2015. Aberrant executive and frontoparietal functional connectivity in very preterm infants with diffuse white matter abnormalities. Pediatr. Neurol 53, 330–337. [PubMed: 26216502]

Irzan H, Molteni E, Hutel M, Ourselin S, Marlow N, Melbourne A, 2021. White matter analysis of the extremely preterm born adult brain. Neuroimage 237, 118112. [PubMed: 33940145]

Author Manuscript Author Manuscript Author Manuscript Author Manuscript

Iwata S, Iwata O, Bainbridge A, Nakamura T, Kihara H, Hizume E, Sugiura M, Tamura M, Matsuishi T, 2007. Abnormal white matter appearance on term FLAIR predicts neuro-developmental outcome at 6 years old following preterm birth. Int. J. Dev. Neurosci 25, 523–530. [PubMed: 17981426]

Iwata S, Nakamura T, Hizume E, Kihara H, Takashima S, Matsuishi T, Iwata O, 2012. Qualitative brain MRI at term and cognitive outcomes at 9 years after very preterm birth. Pediatrics 129, e1138–e1147. [PubMed: 22529280]

Jelescu IO, Veraart J, Adisetiyo V, Milla SS, Novikov DS, Fieremans E, 2015. One diffusion acquisition and different white matter models: how does microstructure change in human early development based on WMTI and NODDI? Neuroimage 107, 242–256. [PubMed: 25498427]

Jensen EA, Dysart K, Gantz MG, McDonald S, Bamat NA, Keszler M, Kirpalani H, Laughon MM, Poindexter BB, Duncan AF, Yoder BA, Eichenwald EC, DeMauro SB, 2019. The diagnosis of bronchopulmonary dysplasia in very preterm infants. An evidence-based approach. Am. J. Respir. Crit. Care Med 200, 751–759. [PubMed: 30995069]

Jeon TY, Kim JH, Yoo SY, Eo H, Kwon JY, Lee J, Lee M, Chang YS, Park WS, 2012. Neurodevelopmental outcomes in preterm infants: comparison of infants with and without diffuse excessive high signal intensity on MR images at near-term-equivalent age. Radiology 263, 518–526. [PubMed: 22403166]

Jespersen SN, Leigland LA, Cornea A, Kroenke CD, 2012. Determination of axonal and dendritic orientation distributions within the developing cerebral cortex by diffusion tensor imaging. IEEE Trans. Med. Imaging 31, 16–32. [PubMed: 21768045]

Jeurissen B, Tournier JD, Dhollander T, Connelly A, Sijbers J, 2014. Multi-tissue constrained spherical deconvolution for improved analysis of multi-shell diffusion MRI data. Neuroimage 103, 411–426. [PubMed: 25109526]

Judas M, Rados M, Jovanov-Milosevic N, Hrabac P, Stern-Padovan R, Kostovic I, 2005. Structural, immunocytochemical, and mr imaging properties of periventricular crossroads of growing cortical pathways in preterm infants. AJNR Am. J. Neuroradiol 26, 2671–2684. [PubMed: 16286422]

Kelly CE, Thompson DK, Chen J, Leemans A, Adamson CL, Inder TE, Cheong JL, Doyle LW, Anderson PJ, 2016. Axon density and axon orientation dispersion in children born preterm. Hum. Brain Mapp 37, 3080–3102. [PubMed: 27133221]

Kelly CE, Thompson DK, Genc S, Chen J, Yang JY, Adamson C, Beare R, Seal ML, Doyle LW, Cheong JL, Anderson PJ, 2020. Long-term development of white matter fibre density and morphology up to 13 years after preterm birth: a fixel-based analysis. Neuroimage 220, 117068. [PubMed: 32585342]

Kidokoro H, Anderson PJ, Doyle LW, Neil JJ, Inder TE, 2011. High signal intensity on T2-weighted MR imaging at term-equivalent age in preterm infants does not predict 2-year neurodevelopmental outcomes. AJNR Am. J. Neuroradiol 32, 2005–2010. [PubMed: 21960493]

Kidokoro H, Neil JJ, Inder TE, 2013. New MR imaging assessment tool to define brain abnormalities in very preterm infants at term. AJNR Am. J. Neuroradiol 34, 2208–2214. [PubMed: 23620070]

Kline JE, Illapani VSP, He L, Altaye M, Logan JW, Parikh NA, 2020a. Early cortical maturation predicts neurodevelopment in very preterm infants. Arch. Dis. Child. Fetal Neonatal. Ed 105, 460–465. [PubMed: 31704737]

Kline JE, Illapani VSP, He L, Altaye M, Parikh NA, 2019. Retinopathy of prematurity and bronchopulmonary dysplasia are independent antecedents of cortical maturational abnormalities in very preterm infants. Sci. Rep 9, 19679. [PubMed: 31873183]

Kline JE, Illapani VSP, Li H, He L, Yuan W, Parikh NA, 2021. Diffuse white matter abnormality in very preterm infants at term reflects reduced brain network efficiency. Neuroimage Clin 31, 102739. [PubMed: 34237685]

Kline JE, Sita Priyanka Illapani V, He L, Parikh NA, 2020b. Automated brain morphometric biomarkers from MRI at term predict motor development in very preterm infants. Neuroimage Clin 28, 102475. [PubMed: 33395969]

Krishnan ML, Dyet LE, Boardman JP, Kapellou O, Allsop JM, Cowan F, Edwards AD, Rutherford MA, Counsell SJ, 2007. Relationship between white matter apparent diffusion coefficients in

Author Manuscript Author Manuscript Author Manuscript Author Manuscript

preterm infants at term-equivalent age and developmental outcome at 2 years. Pediatrics 120, e604–e609. [PubMed: 17698966]

Krishnan ML, Van Steenwinckel J, Schang AL, Yan J, Arnadottir J, Le Charpentier T, Csaba Z, Dournaud P, Cipriani S, Auvynet C, Titomanlio L, Pansiot J, Ball G, Boardman JP, Walley AJ, Saxena A, Mirza G, Fleiss B, Edwards AD, Petretto E, Gressens P, 2017a. Integrative genomics of microglia implicates DLG4 (PSD95) in the white matter development of preterm infants. Nat. Commun 8, 428. [PubMed: 28874660]

Krishnan ML, Wang Z, Aljabar P, Ball G, Mirza G, Saxena A, Counsell SJ, Hajnal JV, Montana G, Edwards AD, 2017b. Machine learning shows association between genetic variability in PPARG and cerebral connectivity in preterm infants. Proc. Natl. Acad. Sci. U.S.A 114, 13744–13749. [PubMed: 29229843]

Kunz N, Zhang H, Vasung L, O'Brien KR, Assaf Y, Lazeyras F, Alexander DC, Huppi PS, 2014. Assessing white matter microstructure of the newborn with multi-shell diffusion MRI and biophysical compartment models. Neuroimage 96, 288–299. [PubMed: 24680870]

Leitner Y, Weinstein M, Myers V, Uliel S, Geva K, Berger I, Marom R, Bashat DB, Ben-Sira L, Geva R, Gross-Tsur V, 2014. Diffuse excessive high signal intensity in low-risk preterm infants at term-equivalent age does not predict outcome at 1 year: a prospective study. Neuroradiology 56, 669–678. [PubMed: 24823447]

Li H, Chen M, Wang J, Illapani VSP, Parikh NA, He L, 2021. Automatic segmentation of diffuse white matter abnormality on T2-weighted brain MR images using deep learning in very preterm infants. Radiol. Artif. Intell 3, e200166. [PubMed: 34142089]

Li H, Parikh NA, Wang J, Merhar S, Chen M, Parikh M, Holland S, He L, 2019. Objective and automated detection of diffuse white matter abnormality in preterm infants using deep convolutional neural networks. Front. Neurosci 13, 610. [PubMed: 31275101]

Maalouf EF, Duggan PJ, Rutherford MA, Counsell SJ, Fletcher AM, Battin M, Cowan F, Edwards AD, 1999. Magnetic resonance imaging of the brain in a cohort of extremely preterm infants. J Pediatr 135, 351–357. [PubMed: 10484802]

Makropoulos A, Gousias IS, Ledig C, Aljabar P, Serag A, Hajnal JV, Edwards AD, Counsell SJ, Rueckert D, 2014. Automatic whole brain MRI segmentation of the developing neonatal brain. IEEE Trans. Med. Imaging 33, 1818–1831. [PubMed: 24816548]

Makropoulos A, Robinson EC, Schuh A, Wright R, Fitzgibbon S, Bozek J, Counsell SJ, Steinweg J, Vecchiato K, Passerat-Palmbach J, Lenz G, Mortari F, Tenev T, Duff EP, Bastiani M, Cordero-Grande L, Hughes E, Tusor N, Tournier JD, Hutter J, Price AN, Teixeira R, Murgasova M, Victor S, Kelly C, Rutherford MA, Smith SM, Edwards AD, Hajnal JV, Jenkinson M, Rueckert D, 2018. The developing human connectome project: a minimal processing pipeline for neonatal cortical surface reconstruction. Neuroimage 173, 88–112. [PubMed: 29409960]

Morel B, Bertault P, Favrais G, Tavernier E, Tosello B, Bednarek N, Barantin L, Chadie A, Proisy M, Xu Y, Bloch I, Sirinelli D, Adamsbaum C, Tauber C, Saliba EEPIRMEX study group, 2021. Automated brain MRI metrics in the EPIRMEX cohort of preterm newborns: Correlation with the neurodevelopmental outcome at 2 years. Diagn. Interv. Imaging 102, 225–232. [PubMed: 33187906]

Mukherjee P, Miller JH, Shimony JS, Conturo TE, Lee BC, Almli CR, McKinstry RC, 2001. Normal brain maturation during childhood: developmental trends characterized with diffusion-tensor MR imaging. Radiology 221, 349–358. [PubMed: 11687675]

Pannek K, George JM, Boyd RN, Colditz PB, Rose SE, Fripp J, 2020. Brain microstructure and morphology of very preterm-born infants at term equivalent age: Associations with motor and cognitive outcomes at 1 and 2 years. Neuroimage 221, 117163. [PubMed: 32663645]

Parikh NA, 2016. Advanced neuroimaging and its role in predicting neurodevelopmental outcomes in very preterm infants. Semin. Perinatol 40, 530–541. [PubMed: 27863706]

Parikh NA, Harpster K, He L, Illapani VSP, Khalid FC, Klebanoff MA, O'Shea TM, Altaye M, 2020a. Novel diffuse white matter abnormality biomarker at term-equivalent age enhances prediction of long-term motor development in very preterm children. Sci. Rep 10, 15920. [PubMed: 32985533]

Parikh NA, He L, Bonfante-Mejia E, Hochhauser L, Wilder PE, Burson K, Kaur S, 2013. Automatically quantified diffuse excessive high signal intensity on MRI predicts cognitive development in preterm infants. Pediatr. Neurol 49, 424–430. [PubMed: 24138952]

Author Manuscript Author Manuscript Author Manuscript Author Manuscript

Parikh NA, He L, Li H, Priyanka Illapani VS, Klebanoff MA, 2020b. Antecedents of objectively diagnosed diffuse white matter abnormality in very preterm infants. Pediatr. Neurol 106, 56–62. [PubMed: 32139164]

Parikh NA, He L, Priyanka Illapani VS, Altaye M, Folger AT, Yeates KO, 2020c. Objectively diagnosed diffuse white matter abnormality at term is an independent predictor of cognitive and language outcomes in infants born very preterm. J. Pediatr 220, 56–63. [PubMed: 32147220]

Parikh NA, Pierson CR, Rusin JA, 2016. Neuropathology associated with diffuse excessive high signal intensity abnormalities on magnetic resonance imaging in very preterm infants. Pediatr. Neurol 65, 78–85. [PubMed: 27567289]

Parikh NA, Sharma P, He L, Li H, Altaye M, Priyanka Illapani VSCincinnati Infant Neurodevelopment Early Prediction Study (CINEPS) Investigators, 2021. Perinatal risk and protective factors in the development of diffuse white matter abnormality on term-equivalent age magnetic resonance imaging in infants born very preterm. J. Pediatr 233, 58–65 e53. [PubMed: 33259857]

Pierson CR, Folkerth RD, Billiards SS, Trachtenberg FL, Drinkwater ME, Volpe JJ, Kinney HC, 2007. Gray matter injury associated with periventricular leukomalacia in the premature infant. Acta Neuropathol 114, 619–631. [PubMed: 17912538]

Raffelt DA, Smith RE, Ridgway GR, Tournier JD, Vaughan DN, Rose S, Henderson R, Connelly A, 2015. Connectivity-based fixel enhancement: whole-brain statistical analysis of diffusion MRI measures in the presence of crossing fibres. Neuroimage 117, 40–55. [PubMed: 26004503]

Rath CP, Desai S, Rao SC, Patole S, 2021. Diffuse excessive high signal intensity on term equivalent MRI does not predict disability: a systematic review and meta-analysis. Arch. Dis. Child. Fetal Neonatal Ed 106, 9–16. [PubMed: 32451357]

Reijmer YD, Leemans A, Heringa SM, Wielaard I, Jeurissen B, Koek HL, Biessels GJVascular Cognitive Impairment Study, g., 2012. Improved sensitivity to cerebral white matter abnormalities in Alzheimer's disease with spherical deconvolution based tractography. PLoS One 7, e44074. [PubMed: 22952880]

Shimony JS, Smyser CD, Wideman G, Alexopoulos D, Hill J, Harwell J, Dierker D, Van Essen DC, Inder TE, Neil JJ, 2016. Comparison of cortical folding measures for evaluation of developing human brain. Neuroimage 125, 780–790. [PubMed: 26550941]

Skiold B, Horsch S, Hallberg B, Engstrom M, Nagy Z, Mosskin M, Blennow M, Aden U, 2010. White matter changes in extremely preterm infants, a population-based diffusion tensor imaging study. Acta Paediatr 99, 842–849. [PubMed: 20132144]

Skiold B, Vollmer B, Bohm B, Hallberg B, Horsch S, Mosskin M, Lagercrantz H, Aden U, Blennow M, 2012. Neonatal magnetic resonance imaging and outcome at age 30 months in extremely preterm infants. J. Pediatr 160, 559–566 e551. [PubMed: 22056283]

Smith SM, Jenkinson M, Johansen-Berg H, Rueckert D, Nichols TE, Mackay CE, Watkins KE, Ciccarelli O, Cader MZ, Matthews PM, Behrens TE, 2006. Tract-based spatial statistics: voxelwise analysis of multi-subject diffusion data. Neuroimage 31, 1487–1505. [PubMed: 16624579]

Soares JM, Marques P, Alves V, Sousa N, 2013. A hitchhiker's guide to diffusion tensor imaging. Front. Neurosci 7, 31. [PubMed: 23486659]

Srinivasan L, Dutta R, Counsell SJ, Allsop JM, Boardman JP, Rutherford MA, Edwards AD, 2007. Quantification of deep gray matter in preterm infants at term-equivalent age using manual volumetry of 3-tesla magnetic resonance images. Pediatrics 119, 759–765. [PubMed: 17403847]

Stoye DQ, Blesa M, Sullivan G, Galdi P, Lamb GJ, Black GS, Quigley AJ, Thrippleton MJ, Bastin ME, Reynolds RM, Boardman JP, 2020. Maternal cortisol is associated with neonatal amygdala microstructure and connectivity in a sexually dimorphic manner. Elife 9, e60729. [PubMed: 33228850]

Tournier JD, Calamante F, Connelly A, 2007. Robust determination of the fibre orientation distribution in diffusion MRI: non-negativity constrained super-resolved spherical deconvolution. Neuroimage 35, 1459–1472. [PubMed: 17379540]

Tournier JD, Calamante F, Gadian DG, Connelly A, 2004. Direct estimation of the fiber orientation density function from diffusion-weighted MRI data using spherical deconvolution. Neuroimage 23, 1176–1185. [PubMed: 15528117]

Author Manuscript Author Manuscript Author Manuscript Author Manuscript

Tournier JD, Smith R, Raffelt D, Tabbara R, Dhollander T, Pietsch M, Christiaens D, Jeurissen B, Yeh CH, Connelly A, 2019. MRtrix3: a fast, flexible and open software framework for medical image processing and visualisation. Neuroimage 202, 116137. [PubMed: 31473352]

Tournier JD, Yeh CH, Calamante F, Cho KH, Connelly A, Lin CP, 2008. Resolving crossing fibres using constrained spherical deconvolution: validation using diffusion-weighted imaging phantom data. Neuroimage 42, 617–625. [PubMed: 18583153]

Valavani E, Blesa M, Galdi P, Sullivan G, Dean B, Cruickshank H, Sitko-Rudnicka M, Bastin ME, Chin RFM, MacIntyre DJ, Fletcher-Watson S, Boardman JP, Tsanas A, 2021. Language function following preterm birth: prediction using machine learning. Pediatr. Res 92, 480–489. [PubMed: 34635792]

Van Essen DC, 1997. A tension-based theory of morphogenesis and compact wiring in the central nervous system. Nature 385, 313–318. [PubMed: 9002514]

Vassar R, Schadl K, Cahill-Rowley K, Yeom K, Stevenson D, Rose J, 2020. Neonatal brain microstructure and machine-learning-based prediction of early language development in children born very preterm. Pediatr. Neurol 108, 86–92. [PubMed: 32279900]

Volpe JJ, 2009. Brain injury in premature infants: a complex amalgam of destructive and developmental disturbances. Lancet Neurol 8, 110–124. [PubMed: 19081519]

Volpe JJ, 2017. Confusions in nomenclature: “periventricular leukomalacia” and “white matter injury”-identical, distinct, or overlapping? Pediatr. Neurol 73, 3–6. [PubMed: 28648484]

Wang Y, Wang Q, Haldar JP, Yeh FC, Xie M, Sun P, Tu TW, Trinkaus K, Klein RS, Cross AH, Song SK, 2011. Quantification of increased cellularity during inflammatory demyelination. Brain 134, 3590–3601. [PubMed: 22171354]

Wheater ENW, Galdi P, McCartney DL, Blesa M, Sullivan G, Stoye DQ, Lamb G, Sparrow S, Murphy L, Wrobel N, Quigley AJ, Semple S, Thrippleton MJ, Wardlaw JM, Bastin ME, Marioni RE, Cox SR, Boardman JP, 2022. DNA methylation in relation to gestational age and brain dysmaturation in preterm infants. Brain Commun 4, fcac056. [PubMed: 35402911]

Young JM, Vandewouw MM, Mossad SI, Morgan BR, Lee W, Smith ML, Sled JG, Taylor MJ, 2019. White matter microstructural differences identified using multi-shell diffusion imaging in six-year-old children born very preterm. Neuroimage Clin 23, 101855. [PubMed: 31103872]

Zhang H, Schneider T, Wheeler-Kingshott CA, Alexander DC, 2012. NODDI: practical *in vivo* neurite orientation dispersion and density imaging of the human brain. Neuroimage 61, 1000–1016. [PubMed: 22484410]

Author Manuscript Author Manuscript Author Manuscript Author Manuscript

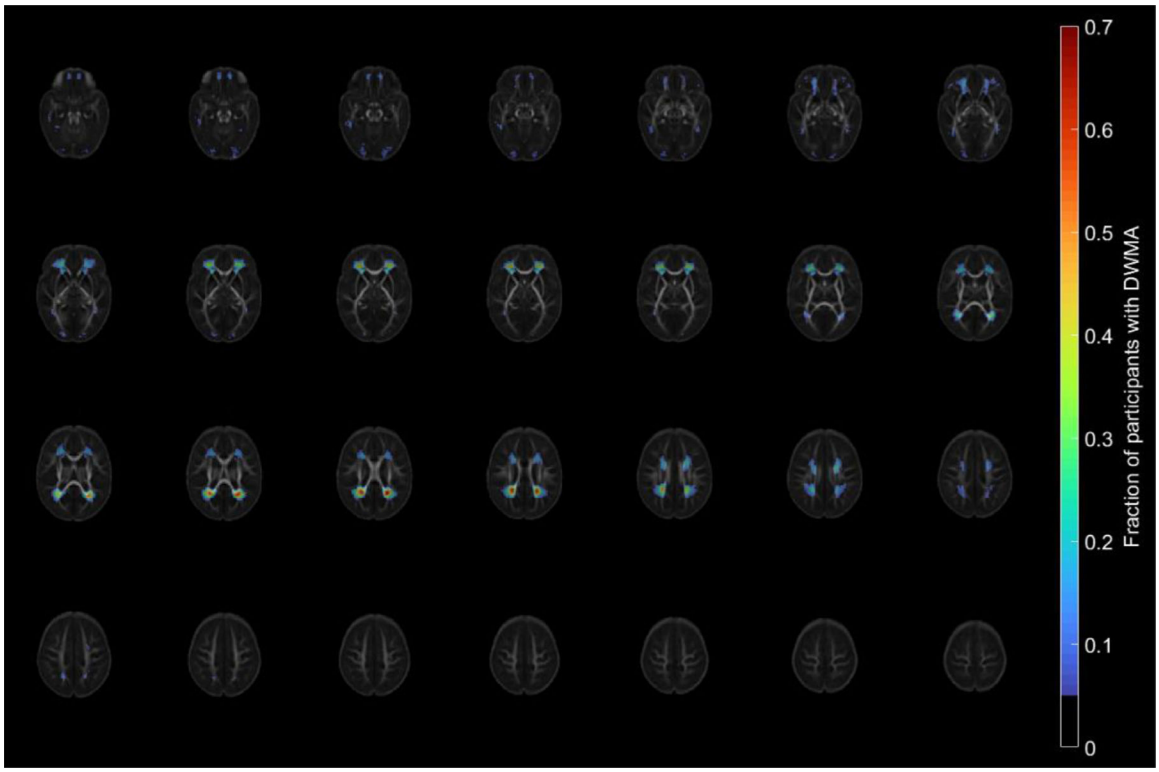

Fig. 1. Heatmap of diffuse white matter abnormality (DWMA) distribution in the preterm brain.
Automated DWMA segmentations for 180 preterm infants created by our deep learning algorithm were aligned to the same template generated by TBSS using linear and nonlinear warping, to produce a heatmap of its prevalence in our cohort.

Author Manuscript Author Manuscript Author Manuscript Author Manuscript

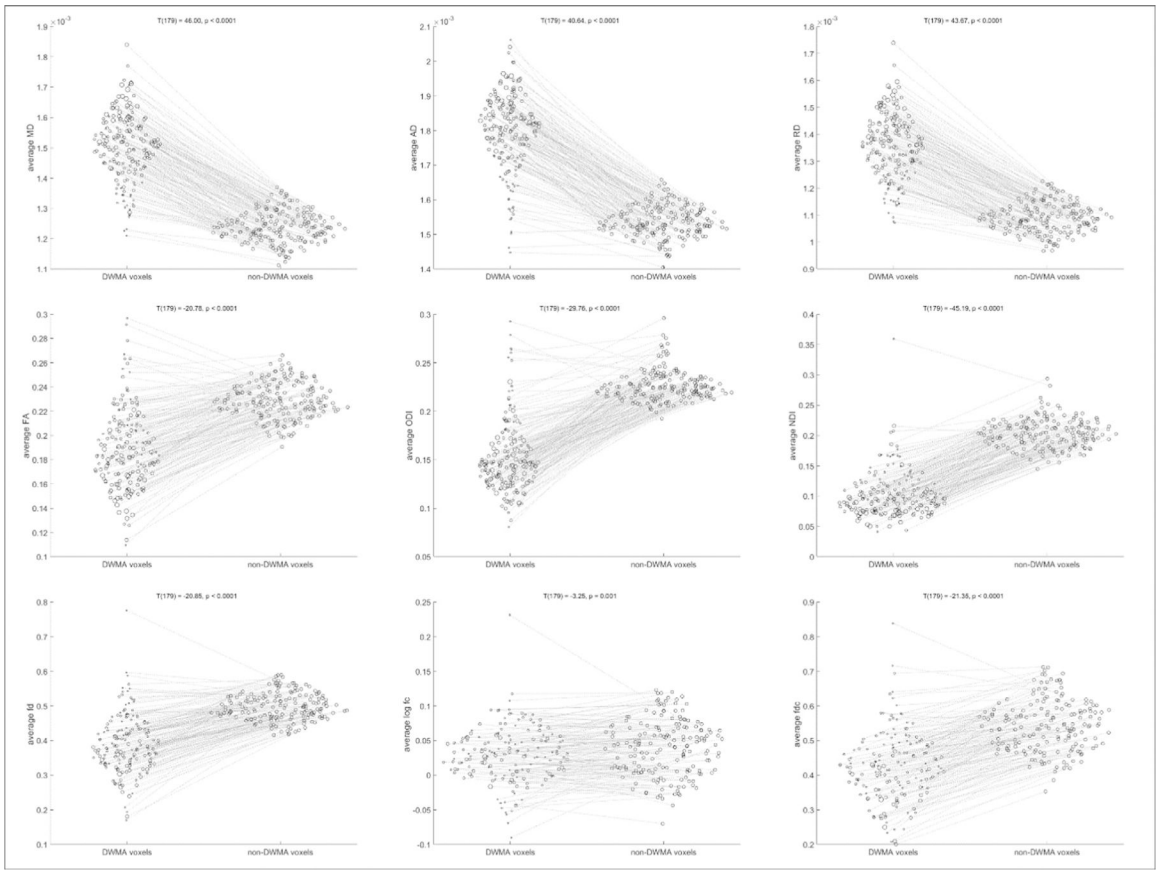

Fig. 2. Average diffusion-weighted imaging-derived metrics for white matter voxels identified as diffuse white matter abnormality (DWMA) compared to non-DWMA white matter voxels.

Metrics are from left to right, top row: mean diffusivity, axial diffusivity, radial diffusivity; middle row: fractional anisotropy, orientation dispersion index, neurite density index; bottom row: mean fiber density, mean log fiber cross-section, and mean fiber density and cross-section. Each line segment represents one participant; the size of the circle at the left end of the line segment is proportional to that participant's total DWMA volume; the size of the circle at the right end of the line segment is not scaled.

Author Manuscript Author Manuscript Author Manuscript Author Manuscript

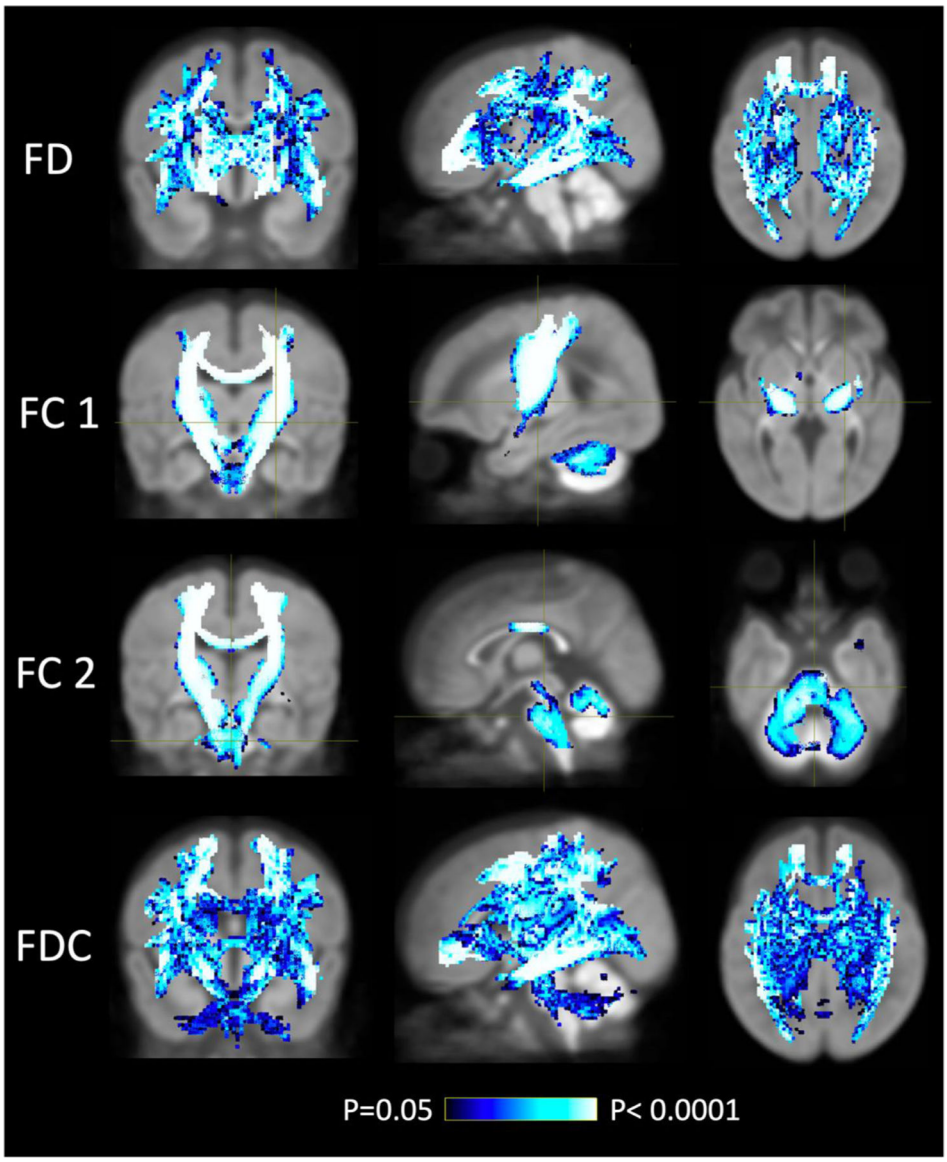

Fig. 3. Relationship between CSD metrics and DWMA extent

Streamlines traversing fixels in which CSD metrics FD, FC, and FDC decreased with DWMA extent. For FD and FDC, all significant regions are shown at once, i.e., the image of the significant streamlines is not dependent on the position of the crosshair. For rows FC 1 and FC 2, the crosshair shows the voxel position on two different views of the same data. The color bar indicates the p-value after family-wise error rate correction.

Author Manuscript Author Manuscript Author Manuscript Author Manuscript

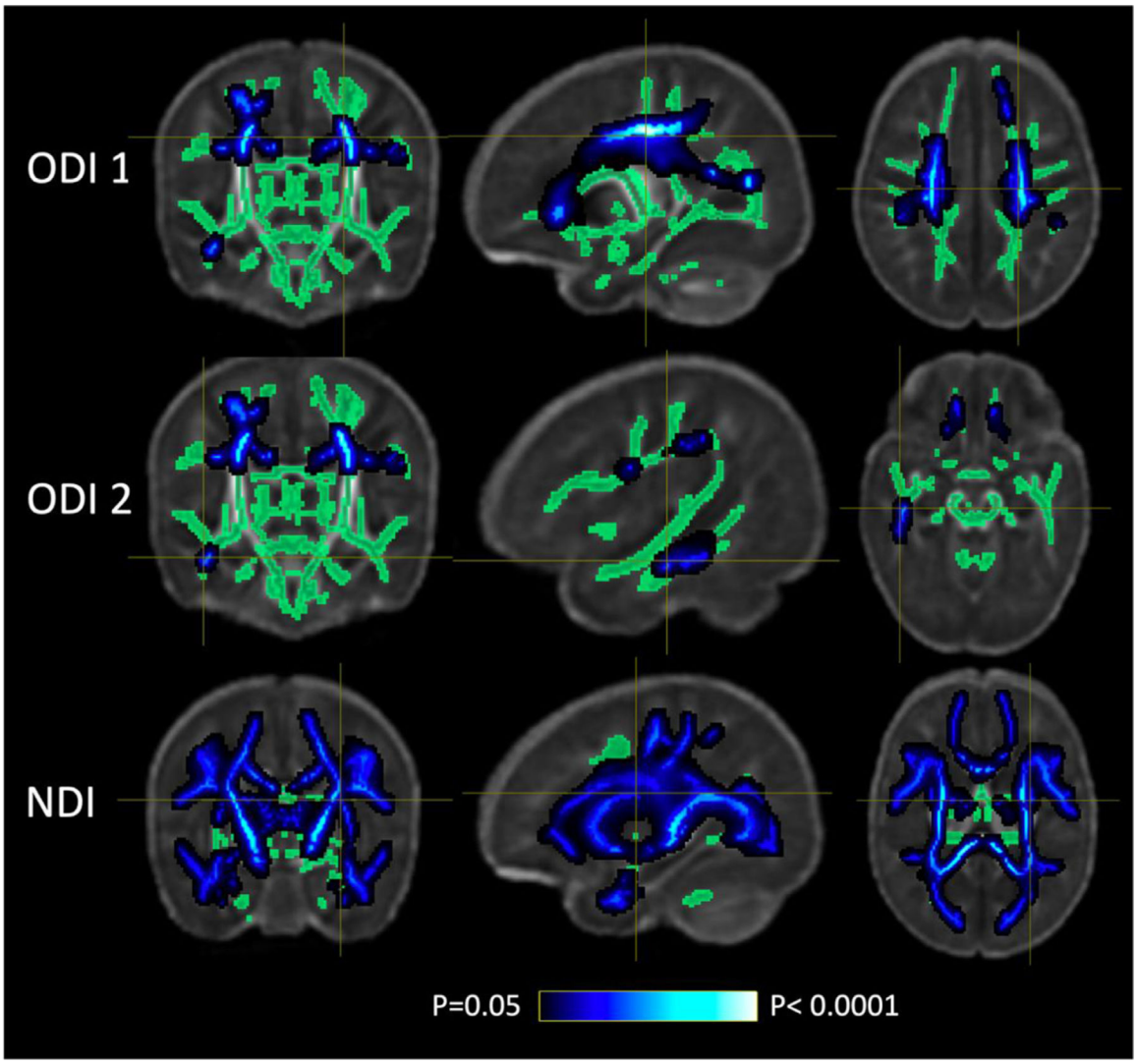

Fig. 4. Relationship between NODDI metrics and DWMA extent.

TBSS results showing white matter regions in which ODI (top two rows) and NDI (bottom row) decreased with DWMA extent. Green areas represent the TBSS white matter skeleton.

Author Manuscript Author Manuscript Author Manuscript Author Manuscript

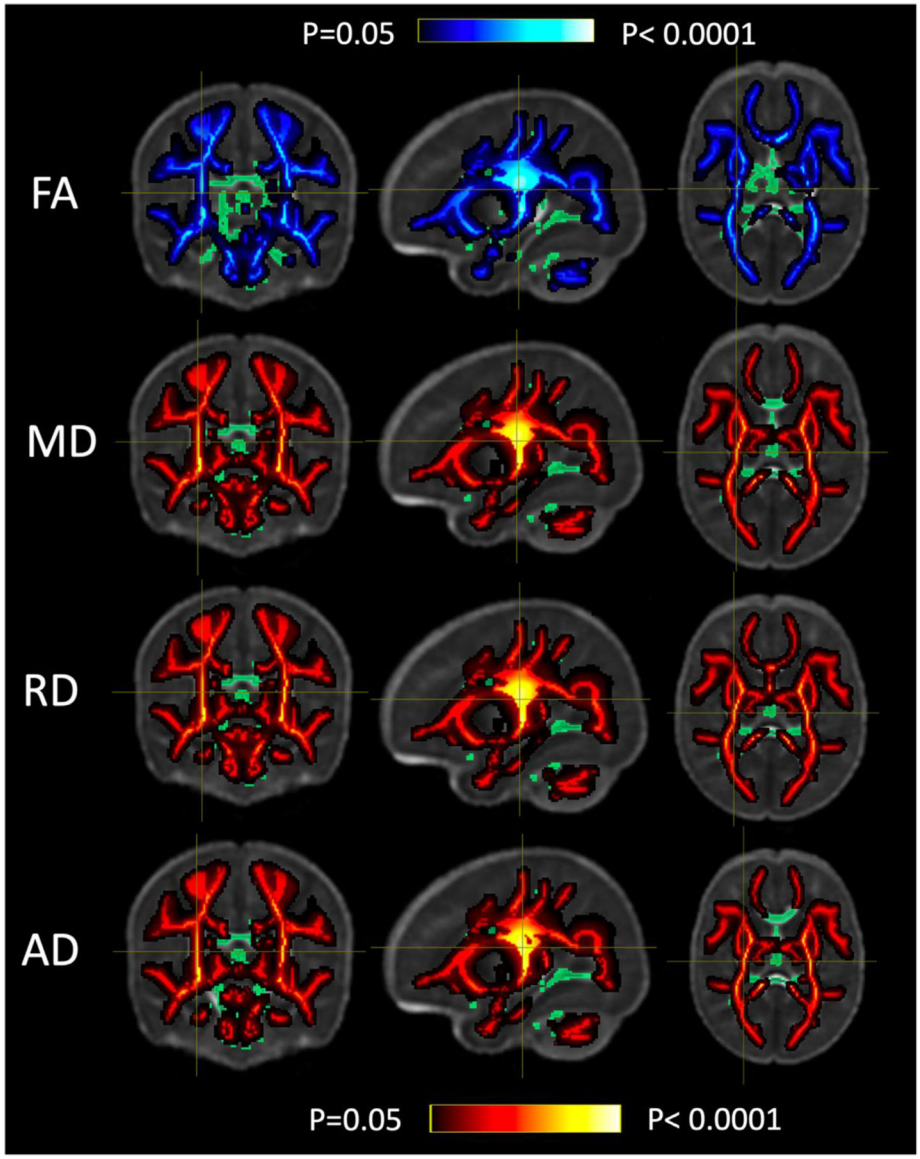

Fig. 5. Relationship between DT metrics and DWMA extent.

TBSS results showing regions in which FA, MD, RD, and AD from the DT model were significantly associated with DWMA extent. Red/blue signifies increase/decrease with DWMA extent. Green areas represent the TBSS white matter skeleton.

Author Manuscript Author Manuscript Author Manuscript Author Manuscript

Neuroimage. Author manuscript; available in PMC 2023 February 08.

Table 1

Baseline and neonatal intensive care characteristic comparisons of the final preterm cohort and the excluded group.

Characteristics	Included (N=180)	Excluded (N=22)	P
Antenatal steroids (completed course), n (%)	165 (91.7)	20 (90.9)	1.00
Maternal magnesium therapy, n (%) *	150 (84.7)	19 (90.5)	0.75
Moderate to severe chorioamnionitis, n (%) **	21 (12.5)	2 (10.0)	1.00
Gestational age, weeks, mean (SD)	29.7 (2.2)	30.5 (2.1)	*0.04*
Birth weight, grams, mean (SD)	1354.0 (415.4)	1546.3 (369.2)	*0.009*
Male, n (%)	95 (52.8)	6 (27.3)	*0.04*
Severe retinopathy of prematurity, n (%)	2 (1.1)	1 (4.5)	0.29
Severe bronchopulmonary dysplasia (BPD), n (%)	18 (10.0)	1 (4.5)	0.70
Caffeine therapy, n (%)	127 (70.6)	16 (72.7)	1.00
Days on supplementary oxygen, mean (SD)	23.0 (31.8)	16.6 (31.9)	0.29
Late onset sepsis, n (%)	11 (6.1)	0 (0)	0.61
Pneumothorax, n (%)	14 (7.8)	1 (4.5)	1.00
Necrotizing enterocolitis	2 (1.1)	0 (0)	1.00
Maternal milk at discharge, n (%)	105 (58.3)	15 (68.2)	0.49
Postnatal dexamethasone for severe BPD, n (%)	7 (3.9)	1 (4.5)	1.00
Caffeine for severe BPD	18 (10.0)	1 (4.5)	0.70
Global brain abnormality score, median (iqr)	3.3 (2.1)	3.7 (2.0)	0.22
White matter abnormality score, median (iqr)	1.6 (1.4)	2.2 (2.0)	0.07
Postmenstrual age at MRI scan, mean (SD)	42.8 (1.3)	42.8 (1.3)	0.43

* 3 included subjects and 1 excluded subject did not have maternal magnesium therapy data.

** 12 included subjects and 2 excluded subjects did not have chorioamnionitis data.